---

**Article:**
Kim, J-Y., Ionescu, A., Mansell, R. et al. (11 more authors) (2017) Structural and magnetic properties of ultra-thin Fe films on metal-organic chemical vapour deposited GaN(0001). Journal of Applied Physics, 121 (4). 043904. ISSN 0021-8979

https://doi.org/10.1063/1.4973956

---

This manuscript was accepted by J. Appl. Phys. Click here to see the version of record.

# Structural and magnetic properties of ultra-thin Fe films on metal-organic chemical vapour deposited GaN(0001)

Jun-young Kim[1,2], Adrian Ionescu[1], Rhodri Mansell[1], Fabrice Oehler[3,4], Christy J. Kinane[5], Joshaniel F. K. Cooper[5], Nina-Juliane Steinke[5], Sean Langridge[5], Romuald Stankiewicz[6], Colin J. Humphreys[3], Russell P. Cowburn[1], Stuart N. Holmes[7] and Crispin H. W. Barnes[1]

[1] Cavendish Laboratory, University of Cambridge, Cambridge CB3 0HE, UK
[2] Department of Physics, University of York, York YO10 5DD, UK
[3] Department of Material Sciences and Metallurgy, University of Cambridge, Cambridge CB3 0FS, UK
[4] CNRS-Laboratorie de Photonique et de Nanostructures, Route de Nozay, 91460 Marcoussis, France
[5] ISIS-STFC, Rutherford Appleton Laboratory, Didcot, OX11 0QX, UK
[6] Ammono S.A.,2 Prusa Str., 00-493 Warsaw, Poland
[7] Toshiba Research Europe Ltd., Cambridge Science Park, Cambridge CB4 0GZ, UK

## ABSTRACT

Structural and magnetic properties of 1-10 nm thick Fe films deposited on GaN(0001) were investigated. *In-situ* reflecting high energy electron diffraction images indicated a α-Fe(110)/GaN(0001) growth of the 3D Volmer-Weber type. The α-Fe(110) XRD peak showed a 1° full-width at half-maximum, indicating ≈ 20 nm grain sizes. A significant reduction in Fe atomic moment from its bulk value was observed for films thinner than 4 nm. Both GaN/Fe interface roughness and Fe film coercivity increased with Fe thickness, indicating a possible deterioration of Fe crystalline quality. Magnetic anisotropy was mainly uniaxial for all films while hexagonal anisotropies appeared for thicknesses higher than 3.7 nm.

## I. INTRODUCTION

Being a close material system to the much-studied Fe/GaAs structures[1–3], Fe/GaN heterostructures provide an exciting test ground for the spin-transport devices. Thanks to the predicted 100 ns spin lifetimes at RT[4] and the thermal stability of the Fe/GaN interface up to 750 ºC,[5] the Fe/GaN heterostructure has become a topic of active research. Moreover, development of GaN light-emitting diode has further bolstered the technological importance of GaN devices.[6]

However, creating a clean, abrupt interface between Fe and GaN for efficient spin injection and detection remains a difficult task. As seen in Fig. 1, large lattice mismatches (- 9.2% along Fe[100] and - 22 % along Fe[111] and Fe[$\bar{1}$11]) between the hexagonal GaN(0001) and the cubic α-Fe(110) complicate the growth process and result in non-trivial orientation relationships. Previous electron backscatter diffraction studies of Fe films on GaN(0001) demonstrated α-Fe(110) growth, where the large in-plane lattice mismatches were compensated by forming three degenerate in-plane crystal domains rotated 120 degrees from each other, as in

$\alpha - \mathrm{Fe}(110)\langle 001\rangle \,||\, \mathrm{GaN}(0001)\langle 11\bar{2}0\rangle$.[7] Furthermore, a study by Wong *et al.* indicated a Volmer-Weber type growth where the Fe growth proceeded by forming three-dimensional islands.[8] The same authors also observed clear reflecting high-energy electron diffraction (RHEED) streaks after 10 monolayers (MLs) of Fe deposition, indicating an epitaxial Fe(110) growth. In addition, the magnetic anisotropy of the Fe films was found to change from perpendicular to in-plane directions after 4.5 ML Fe deposition,[9] and a hexagonal in-plane anisotropy was observed for the Fe films thicker than 5 nm.[10]

One problem not discussed in previous papers was that typical GaN layers grown on $Al_2O_3(0001)$ are heavily strained due to the large lattice and thermal mismatch between GaN and sapphire. This strain is then translated through magnetostriction into the total magnetic anisotropy of the Fe films. Hence, a direct comparison between the studies of different types of GaN is not straightforward.

In this paper, we aim to provide a benchmark for a near strain-free Fe/GaN system, as confirmed by optical curvature measurements. Structural properties of 1-10 nm thick MBE-deposited Fe films on GaN(0001) were investigated by using *in-situ* RHEED, X-ray reflection and diffraction (XRR/XRD). The magnetic hystereses and anisotropies of the Fe films were examined using magneto-optic Kerr effect (MOKE), superconducting quantum interference device (SQUID) and vibrating sample magnetometer (VSM) magnetometry. Furthermore, the saturation magnetisation of the ultra-thin (< 5 nm) Fe films was estimated by polarised neutron reflectometry (PNR).

## II. CURVATURES

Our pilot study using Fe films deposited on hydride vapour phase epitaxy (HVPE) GaN(0001) substrates revealed large convex curvatures (≈ - 0.2 $m^{-1}$) of the deposited Fe films, which complicated X-ray and neutron reflection measurements. The high curvatures of the GaN layer were previously found to be due to the large lattice (≈ - 33%)[11] and thermal[12] mismatches at the $Al_2O_3(0001)$/GaN(0001) interface. In order to find more suitable types of GaN substrates for our purposes, a Multiple Optical Scanner Ultra Scan (k-Space Associates) was used to characterise the surface curvatures of three different GaN substrates as displayed in Fig. 2. Among the HVPE, metal-organic chemical vapour deposition (MOCVD) and ammonothermal bulk GaN(0001) substrates, the bulk substrates showed the smallest values of curvature (< 0.01 $m^{-1}$) while the HVPE recorded the highest values (- 0.16 ± 0.04 $m^{-1}$). Due to the small size of commercially available ammonothermal bulk GaN substrates, a MOCVD GaN layer deposited on 2'' sapphire was specially grown with a - 0.03 ± 0.01 $m^{-1}$ curvature to reduce magnetostriction effects and to allow for reflectivity measurements. Fig. 2(b) shows the horizontal curvature map of the MOCVD GaN on sapphire substrate.

## III. Fe GROWTH

The MOCVD GaN(0001) substrates used in this work were prepared by depositing a 2.1 μm thick GaN layer by MOCVD on a 2-inch *c*-plane sapphire $Al_2O_3$(0001) substrate. *In-situ* optical measurements and the atomic force microscopy on the deposited GaN film showed the radius of curvature of 62.5 m and the threading dislocation density of $2 \times 10^9$ $cm^{-2}$, respectively. Before being loaded in the MBE growth chamber, the GaN substrates were cleaned chemically using acetone, isopropanol and de-ionised water to remove dirt and organic residues. For the 1.5 nm and 3.7 nm samples, additional treatments with hydrochloric acid and buffered hydrofluoric acid solutions were performed for surface oxide removal. However, the additional treatments did not significantly improve the GaN RHEED patterns. The loaded substrates were then heated to 200 °C in ultra-high vacuum (UHV) for two hours to remove the water adsorbed on the surface.

The deposition of the Fe films was performed at room temperature by direct electron-beam sublimation of an Fe source of a 99.99% purity. The base and growth pressure of the chamber were $5 \times 10^{-10}$ mbar and $1 \times 10^{-9}$ mbar, respectively. A typical deposition rate was kept at ≈ 0.14 nm per minute, measured by an *in-situ* quartz microbalance and calibrated against XRR measurements. The deposited Fe layers were capped with Au or Cu layers to prevent oxidation of the Fe films during *ex-situ* measurements.

The *in-situ* RHEED measurements monitored surface crystalline orders of GaN and Fe surfaces during the growth, as shown in Fig. 3. All patterns were recorded with an incident electron beam along the *a*-axis [11-20] of GaN(0001). As shown in inset (a), the GaN(0001) surface showed clear 1 x 1 RHEED pattern with Kikuchi arcs indicative of a smooth and long-range ordered crystalline surface. Along the insets (b) to (e), the Fe thickness increased from 0.14 nm to 1 nm while RHEED patterns became weaker and more blurred, being almost absent at 1 nm. The disappearance of the RHEED patterns suggested a 3D Volmer-Weber type islands growth of the Fe films.[8,13] RHEED streaks re-emerged when thickness increased to above 2 nm as shown in insets (f-i). The streaks were broader than the original GaN streaks. Two separate sets of the observed streaks indicated two different long-range in-plane periodicities of the Fe films. The in-plane periodicities of the Fe films were estimated by measuring the inter-streak distances of the Fe RHEED and comparing with those of the original GaN(0001) streaks. Assuming the atomic row spacing of 2.74 Å along the *a*-axis of GaN(0001) substrate, two atomic periodicities of the Fe films were estimated to be 2.3 ± 0.1 Å and 2.0 ± 0.1 Å along the same crystalline direction. These values corresponded to atomic periodicities present in Nishiyama-Wasserman ( $\alpha-\mathrm{Fe}(110)\langle 001\rangle \,||\, \mathrm{GaN}(0001)\langle 11\bar{2}0\rangle$ ) and Kurdjumov-Sachs ( $\alpha-\mathrm{Fe}(110)\langle 1\bar{1}1\rangle \,||\, \mathrm{GaN}(0001)\langle 11\bar{2}0\rangle$ ) orientation relations (ORs). From the previous

study of Fe films on Ga- and N-terminated GaN(0001) substrates,[7] Nishiyama-Wasserman OR was expected for our films, as our GaN(0001) layers were prepared to be Ga-terminated. Due to the limited resolution of our RHEED patterns, it was not possible to distinguish between the two ORs in our films from atomic periodicities alone.

## IV. X-RAY DIFFRACTION/REFLECTION

Figure 4 shows an out-of-plane XRD plot of the 10 nm Fe film. A broad peak of α-Fe(110) was observed at a 2θ value of ≈ 45°. The full-width at half-maximum of the α-Fe(110) peak was measured to be around 1°, which corresponded to a typical size of 20 nm for the in-plane crystalline domains according to the Scherrer formula. This XRD measurement agreed well with the higher limit of the domain sizes (≈ 30 nm) estimated previously from electron backscatter measurement.[7] In addition, a small peak at 2θ = 64.7° was inferred to be a superposition of a weak α-Fe(002) peak (at 2θ = 65.2°) with a low intensity diffraction peak of the sharp $Al_2O_3$(0009) reflection (at 2θ = 64.5°). The intensity of the Fe(002) peak was only 5 % of that of the Fe(110) peak, suggesting that the Fe growth was pre-dominantly in the (110) direction.

In Fig. 5(a), a XRR measurement of the 10 nm Fe film on MOCVD GaN(0001) exhibited clear Kiessig fringes from the thickness of the Fe layer. A slab-model fitting using the Bruker Leptos software was applied to analyse the XRR data to obtain the thickness and roughness values of the layers. In Fig. 5(b), the GaN/Fe interface roughness is plotted against Fe thickness, where a general trend of increasing roughness with thickness was observed. One possible cause for this trend of increasing roughness with increasing thickness was that thicker deposited layers caused the Fe atoms at the GaN/Fe interface to be more relaxed, which in turn resulted in higher strains and roughness at the interface. This increase in roughness could also be accountable for the increase in Fe film coercivity as discussed later in this manuscript. The high interface roughness of the 5 nm Fe sample was likely to be due to its especially thick (≈ 70 nm) Cu capping layer, as compared to 3-5 nm capping layer thicknesses of the other films. Further cross-sectional transmission electron microscopy measurements would enable a direct, atomic-scale investigation of the GaN/Fe interface.

## V. SATURATION MAGNETISATION

In order to investigate effects of the Fe/GaN interface on magnetic properties of the Fe films, SQUID and VSM measurements were used to characterise magnetic hysteresis loops. The representative hysteresis loops of the 2.5, 7 and 10 nm samples are shown in Fig. 6(a). From the plots, an increase in saturation magnetisation and coercivity with film thickness could be observed. Figure 6(b) plots the Fe saturation magnetisation $M_S$ per unit area with Fe thickness. A linear fit through the data points yielded a gradient of 1,670 ± 50 emu $cm^{-3}$, which was close to the bulk value of 1,714

emu $cm^{-3}$ for α-Fe.[14] By extrapolating the obtained linear fit, the onset of in-plane ferromagnetism at RT could be predicted to be at around 0.7 ± 0.2 nm, which was in agreement with the onset-point (≈ 0.6 nm) obtained in the previous *in-situ* surface MOKE study.[9]

In order to study the magnetic moment of the films in more detail, PNR measurements were performed for 1 nm, 1.5 nm and 2.5 nm films at RT in an in-plane field of 2.5 kOe at the CRISP beamline in ISIS, Rutherford Appleton Laboratory. Figure 7(a) shows a representative plot of the PNR measurements of the 2.5 nm film. The fits to the data were created using the GenX software.[15] While the data and the fits appeared to agree well, the obtained Fe layer thicknesses were significantly larger (between 3.2 nm and 4.5 nm) than the values from the earlier XRR measurements. By introducing a non-magnetic interface layer between GaN and Fe with an arbitrary thickness in the PNR model, it was possible to retrieve the design Fe thickness values. The thickness of these interface layers varied from 0 nm up to 2.0 nm. However, these interface layers were not observed in our XRR measurements, and for the case of the 2.5 nm film, the 2.0 nm interface layer was as thick as the Fe layer itself. Furthermore, the magnetisation data in Fig. 6(b) suggested the 0.7 nm thick interface layer for all films. The discrepancy between the PNR and the XRR data could be due to the convex curvature of the samples, diverging the reflected beams. Future cross-sectional transmission electron microscopy measurements could verify the exact nature of the interface layer.

Figure 7(b) displays the saturation magnetisation per unit volume of Fe, calculated from the SQUID, VSM and PNR measurements. For the PNR data, the model with the non-magnetic interface layer was used. For films thicker than 5 nm, the moments were close to the bulk α-Fe value of 2.18 $\mu_B$/atom. Films thinner than 4 nm showed a rapid reduction in moment with thickness, where films with thickness below 2 nm displayed moments below half of the bulk value. The noticeable reductions of PNR magnetic moments for the 1.5 nm and 2.5 nm films compared to the value from the VSM measurements could have risen from the sample curvature. According to the analysis from Laloë *et al.*,[16] the decrease in moment with thickness could be modelled with the following formula:

$$\mu_{Fe}^{RT} = 2.18\ [\mu_B/\text{atom}] + \frac{A}{t_{Fe}}[\text{nm} \times \mu_B/\text{atom}] \qquad (1)$$

where $\mu_{Fe}^{RT}$ is the Fe moment per unit volume, $t_{Fe}$ is the Fe thickness and the parameter $A$ can be referred to as the effect from the GaN/Fe interface. The value of $A$ for our films was fitted to be – 1.5 ± 0.2. (The 3.7 nm film was excluded from the fit due to its long (≈ 3 hours) growth time for *in-situ* MOKE measurements.) The value of $A$ for our Fe films was comparably larger than the values of - 0.47 for Fe/GaAs(001) and - 1.14 for Fe/InAs(001).[16] The greater effect of the interface in the α-Fe(110)/GaN(0001) system was thought to be due to the larger lattice mismatch (- 9% along Fe[100] and - 22% along Fe[111]), as compared to 1.6% of Fe/GaAs(001) and -

5.4% of Fe/InAs(001) systems. From our earlier XRR measurements, the GaN/Fe interface roughness in our films (0.6 ± 0.4 nm) was found to be higher than that of the Fe/GaAs(001) (0.3 ± 0.2 nm) and was comparable to that of the Fe/InAs(001) system (0.6 ± 0.2 nm).[16] Higher interface roughness could lead to an increased atomic interdiffusion at the GaN/Fe interface. The formation of non-magnetic alloy at the interface, in turn, would be responsible for the observed reduction of the Fe moment in our films.

## VI. COERCIVITY AND MAGNETIC ANISOTROPY

Fig. 8(a) - (d) show MOKE hysteresis loops of 1.5 nm, 2.5 nm, 7 nm and 10 nm Fe films at 0º - 90° sample angles. For the thinnest (1.5 nm) film, the hysteresis loops gradually changed from a hard-axis switching at 0º to an easy-axis switching at 90° sample angle. A similar trend was seen with the 2.5 nm film, while the observed loops showed a higher squareness than the 1.5 nm film. With the 7 nm film, the hard-to-easy transition with sample angles was less clear, and the 10 nm film showed only easy-axis switching with different coercivities depending on the sample angle. It was also noticed that the coercivity increased with the film thickness, which was counter-intuitive considering the expected lattice relaxation of the thicker Fe films. This increase in coercivity coincided with our earlier observation of increased GaN/Fe interface roughness with film thickness. This increase in the Fe film coercivity was observed previously,[8] where a possible deterioration of the Fe crystalline quality with thickness was suggested as a cause for the observed trend.

In order to investigate the magnetic anisotropy of our films further, remanence measurements were taken using RT VSM magnetometry at different sample angles. Figure 9(a) - (f) display the transverse components of remnant magnetisations, which turned out to be a more sensitive indicator of angular anisotropy than the longitudinal remanence due to its larger variation in values with respect to its base value depending on angle. As can be seen in the Fig. 9(a) and 9(b), the 1.5 nm and the 2.5 nm films showed a uniaxial and a skewed uniaxial angular response. The films thicker than 3.7 nm (Fig. 9(c) – (f)) all showed hexagonal responses, with a varying degree of uniaxial component. The six-fold magnetic anisotropy was expected from the near-hexagonal atomic plane of α-Fe(110), as observed by Gao *et al.*[17] When fully relaxed, the hexagonal α-Fe(110) lattice is expected to be more elongated in Fe[100] directions than in Fe[111] directions, with corresponding lattice parameters of 2.87 Å and 2.48 Å (See Fig. 1). The elongated lattice, with any non-equal distributions of the three crystalline domains, could be a cause for the observed mixture of the uniaxial and six-fold anisotropies. Electron back-scatter diffraction measurements, as employed in Ref. 17, can be insightful in determining the distributions of the crystalline domains in our films.

The films that showed the six-fold symmetries had their magnetic easy axes along the *m*-axes $\langle 1\bar{1}00 \rangle$ of GaN(0001), which was in agreement with a recent study of in-plane anisotropies of α-Fe(110) films on GaN(0001).[18] It is worth noting that the mainly-hexagonal magnetic anisotropy of our 5 nm film was qualitatively different to a dominantly uniaxial behaviour of a 5 nm Fe / 2 nm MgO / MOCVD GaN(0001) system as observed by Khalid *et al.*[19] This change in anisotropy indicated the effect of the bottom interfaces on the in-plane magnetic anisotropy of the Fe films.

## VII. CONCLUSION

In conclusion, we demonstrated an epitaxial growth of α-Fe(110) films by MBE on nearly strain-free MOCVD GaN(0001) substrates. The GaN/Fe interface roughness was found to increase with Fe film thickness, which could be accountable for the observed increase in coercivity. In addition, the Fe layer moment decreased significantly from its bulk value of 2.18 $\mu_B$/atom for the films thinner than 4 nm. Atomic interdiffusion at the GaN/Fe interface due to roughness could be responsible for the observed reduction of the Fe moment. Angular remanence measurements showed the change in the Fe magnetic anisotropy from uniaxial for films thinner than 5 nm to the mixture of uniaxial and hexagonal for the thicker films. This study is the first to investigate systematically the changes in Fe magnetic moment and in-plane magnetic anisotropy in correlation with the thickness of ultra-thin (< 10 nm) Fe films on GaN(0001). It is expected to contribute towards the realisation of future Fe/GaN spintronic devices.[20]

## ACKNOWLEDGEMENTS

Dr A. Blackburn from Hitachi Cambridge Laboratory helped us with the kSA MOS Ultra Scan for curvature measurements. J.K. acknowledges financial aid from Cambridge Overseas Trust.

## REFERENCES

[1] G. Wastlbauer and J. A. C. Bland, Adv. Phys. **54**, 137 (2005).

[2] A. Ionescu, M. Tselepi, D.M. Gillingham, G. Wastlbauer, S. J. Steinmüller, H. E. Beere, D. A. Ritchie, and J. A. C. Bland, Phys. Rev. B **72**, 1 (2005).

[3] L. R. Fleet, K. Yoshida, H. Kobayashi, Y. Kaneko, S. Matsuzaka, Y. Ohno, H. Ohno, S. Honda, J. Inoue, and A. Hirohata, Phys. Rev. B **87**, 1 (2013).

[4] S. Krishnamurthy, M. Van Schilfgaarde, and N. Newman, Appl. Phys. Lett. **83**, 1761 (2003).

[5] C. Gao, O. Brandt, H. P. Schönherr, U. Jahn, J. Herfort, and B. Jenichen, Appl. Phys. Lett. **95**, 2 (2009).

[6] "The Nobel Prize in Physics 2014". Nobelprize.org. Nobel Media AB 2014. Web. 5 Jun 2016. <http://www.nobelprize.org/nobel_prizes/physics/laureates/2014/>.

[7] C. Gao, O. Brandt, S. C. Erwin, J. Lähnemann, U. Jahn, B. Jenichen, and H.P. Schönherr, Phys. Rev. B **82**, 1 (2010).

[8] P. K. J. Wong, W. Zhang, X. Cui, I. Will, Y. Xu, Z. Tao, X. Li, Z. Xie, and R. Zhang, Phys. Status Solidi Appl. Mater. Sci. **208**, 2348 (2011).

[9] K. He, L.Y. Ma, X.C. Ma, J.F. Jia, and Q.K. Xue, Appl. Phys. Lett. **88**, (2006).

[10] R. Meijers, R. Calarco, N. Kaluza, H. Hardtdegen, M. V. D. Ahe, H. L. Bay, H. Lüth, M. Buchmeier, and D. E. Bürgler, J. Cryst. Growth **283**, 500 (2005).

[11] R. Dwiliński, R. Doradziński, J. Garczyński, L. P. Sierzputowski, A. Puchalski, Y. Kanbara, K. Yagi, H. Minakuchi, and H. Hayashi, J. Cryst. Growth **311**, 3015 (2009).

[12] M. Leszczynski, T. Suski, H. Teisseyre, P. Perlin, I. Grzegory, J. Jun, S. Porowski, and T.D. Moustakas, J. Appl. Phys. **76**, 4909 (1994).

[13] Y. Honda, S. Hayakawa, S. Hasegawa, and H. Asahi, Appl. Surf. Sci. **256**, 1069 (2009).

[14] R.M. Bozorth, *Ferromagnetism* (Wiley-IEEE Press, 1993).

[15] Matts Björck, <genx.sourceforge.net>.

[16] J.-B. Laloë, F. Belle, A. Ionescu, C. A. F. Vaz, M. Tselepi, G. Wastlbauer, R. M. Dalgliesh, S. Langridge, J. A. C. Bland, IEEE Trans. Magn. **42**, 2933 (2006).

[17] C. Gao, O. Brandt, J. Lähnemann, J. Herfort, H.-P. Schönherr, U. Jahn, and B. Jenichen, J. Cryst. Growth **323**, 359 (2011).

[18] C. Gao, C. Dong, C. Jia, D. Xue, J. Herfort, and O. Brandt, Phys. Rev. B **92**, 1 (2015).

[19] N. Khalid, J.-y. Kim, A. Ionescu, T. Hussain, F. Oehler, T. Zhu, R. Oliver, I. Farrer, R. Ahmad, C. H. W. Barnes, Submitted to Journal of Magnetism and Magnetic Materials (2016).

[20] S. Fernandez-Garrido, K. U. Ubben, J. Herfort, C. Gao, and O. Brandt, Appl. Phys. Lett. **101**, (2012).

This manuscript was accepted by J. Appl. Phys. Click here to see the version of record.

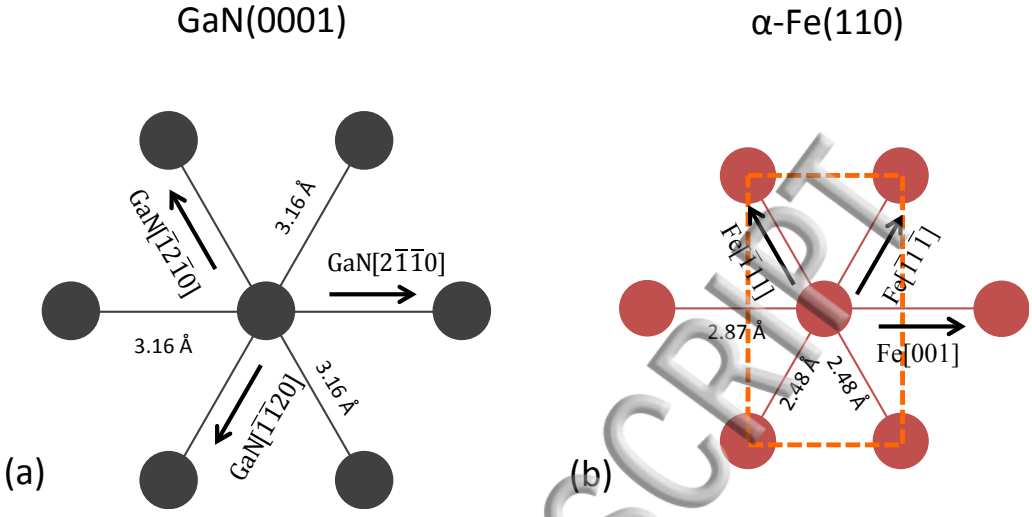


FIG. 1. Schematics of (a) GaN(0001) and (b) α-Fe(110) lattice planes.

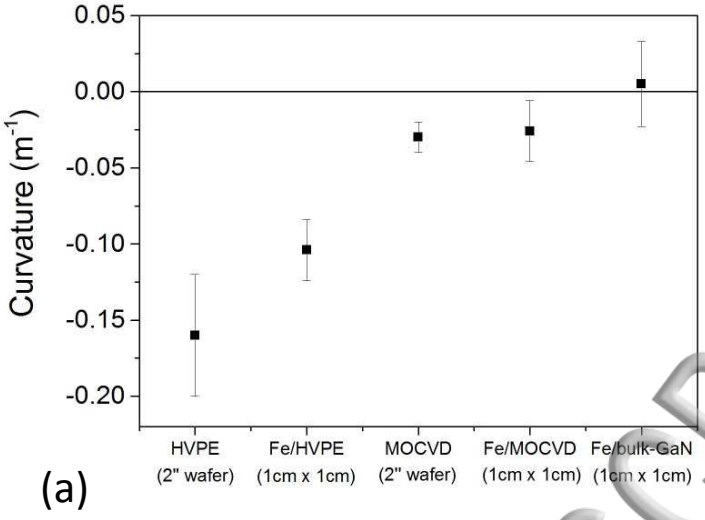


(a)

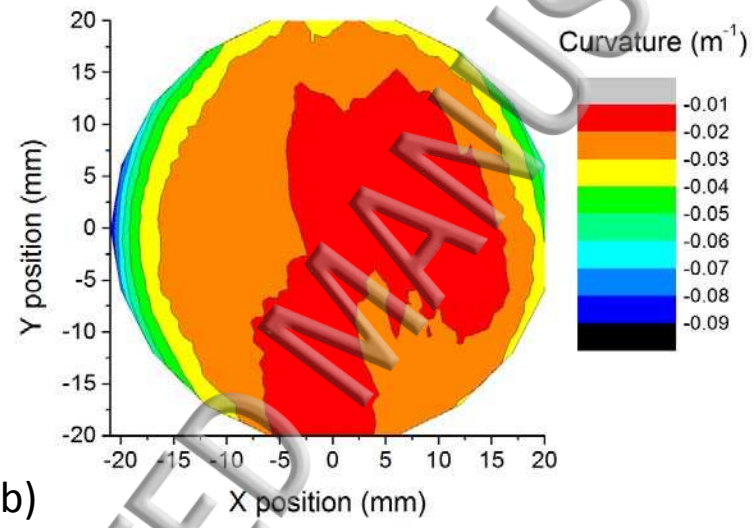


(b)

FIG. 2. (a) Optical curvatures of HVPE, MOCVD and bulk GaN(0001) substrates with and without Fe layers, using a kSA MOS Ultra Scan. (b) Curvature measurement of a 2-inch MOCVD GaN substrate used in this experiment.

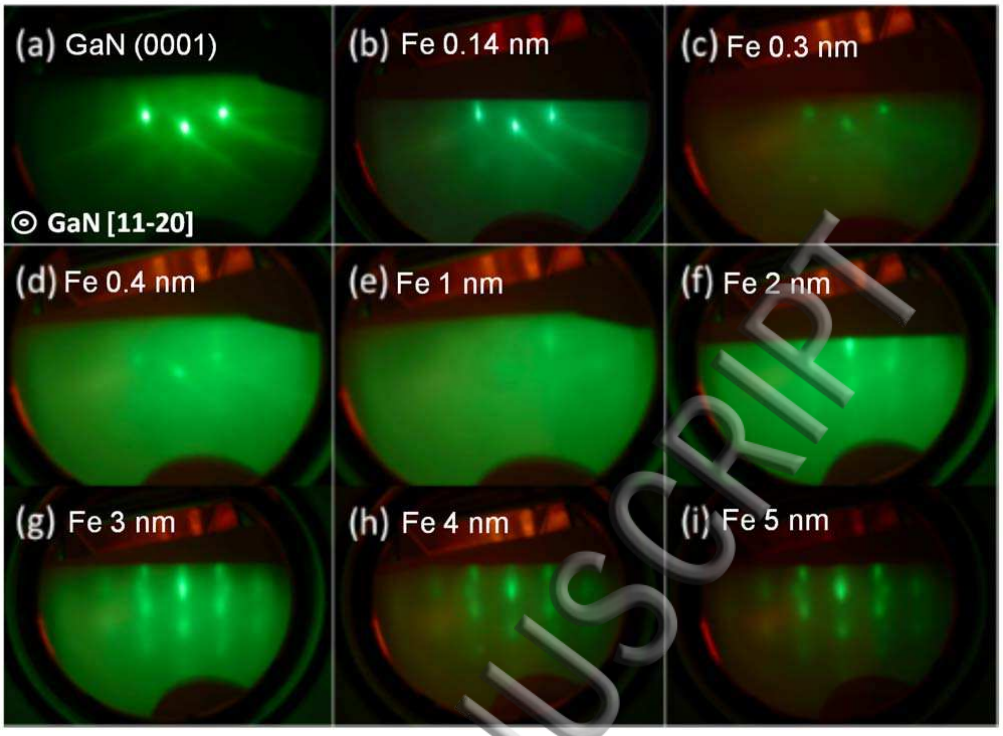


FIG. 3. RHEED images of Fe films on MOCVD GaN(0001) taken with a 15 keV beam energy. (a) The GaN(0001) substrate, (b) after 0.14 nm Fe, (c) 0.28 nm, (d) 0.43 nm, (e) 1 nm, (f) 2 nm, (g) 3 nm, (h) 4 nm and (i) 5 nm. The images were taken along the $[11\bar{2}0]$ direction of the GaN(0001).

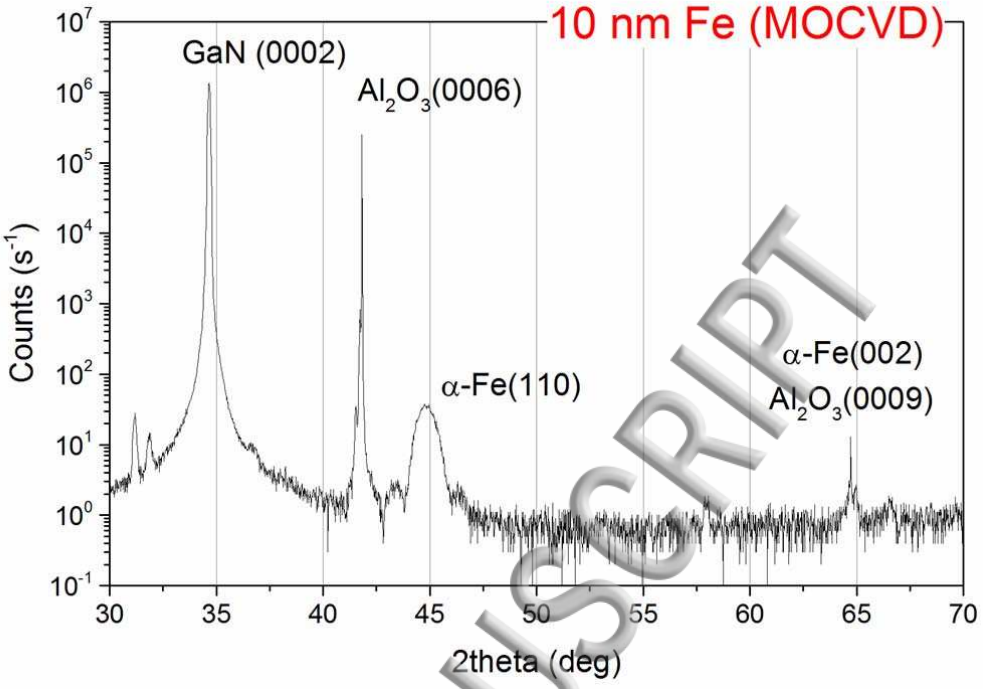


FIG. 4. Out-of-plane XRD measurement of the 10 nm Fe film. The peaks are marked with the corresponding Miller indices.

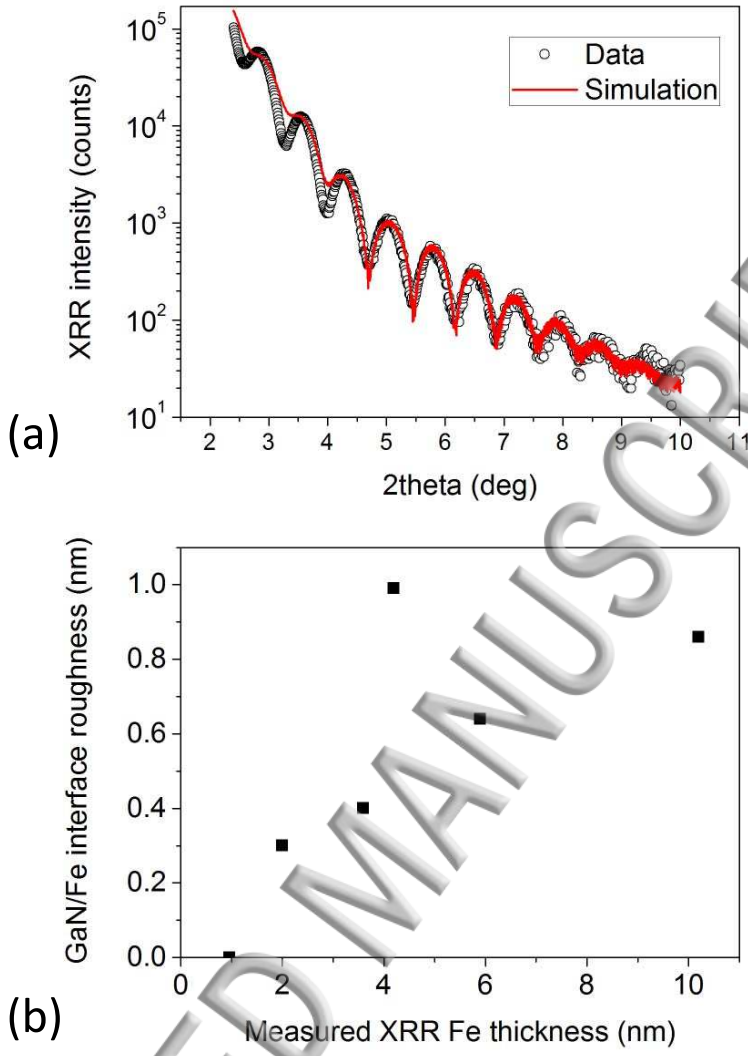


FIG. 5. (a) Representative XRR data and fit for the 10 nm Fe film on MOCVD GaN(0001). (b) GaN/Fe interface roughness with Fe thickness as obtained from XRR measurements.

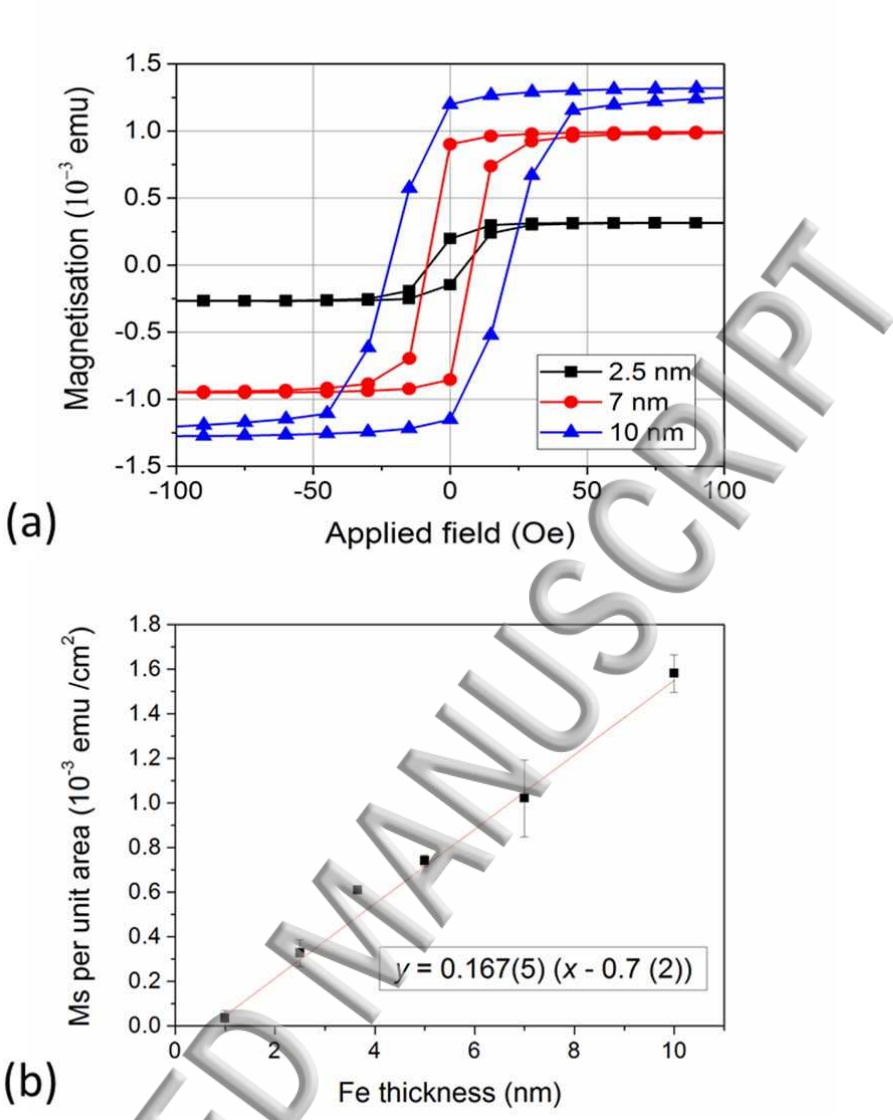


FIG. 6. (a) Representative hysteresis loops of 2.5, 7 and 10 nm samples as measured by VSM along the *a*-axis [11$\bar{2}$0] of GaN(0001). (b) Saturation magnetisation of Fe films per unit area plotted against thickness.

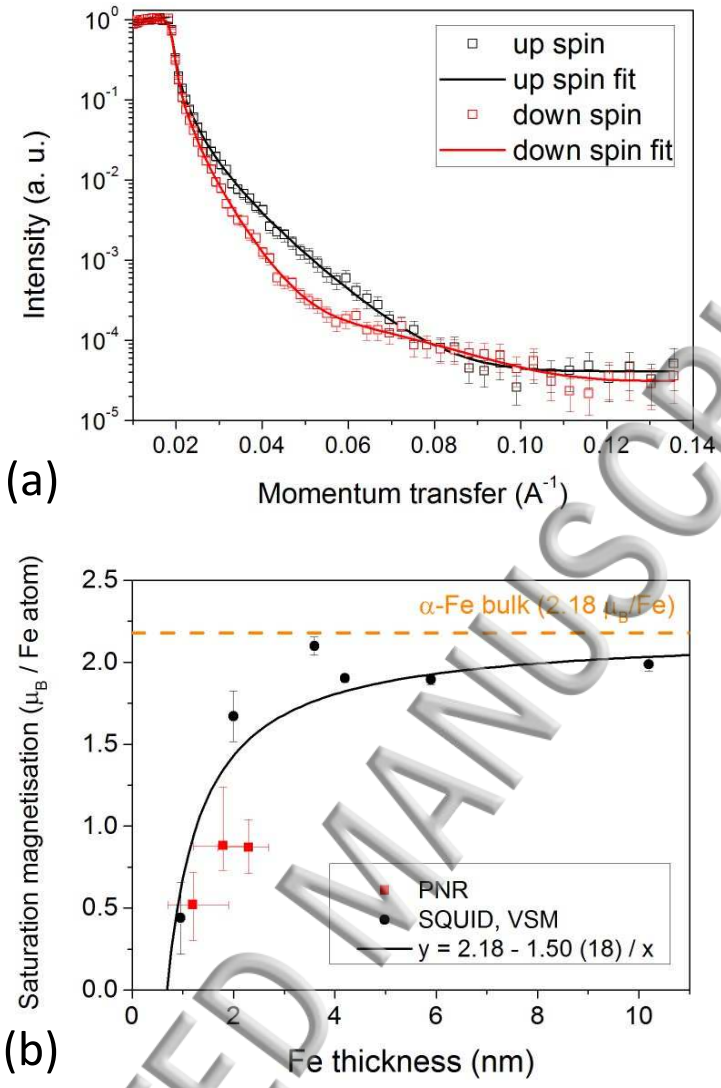


FIG. 7. (a) A representative PNR data and fit for the 2.5 nm sample. (b) A plot of Fe magnetic moment per atom with thickness. The orange (dashed) line displays the bulk α-Fe moment of 2.18 $\mu_B$/atom. The 3.7 nm film was excluded when calculating the black curve line fit, as this film was left in the chamber without the Au capping considerable longer (3 hours) for *in-situ* MOKE measurements.

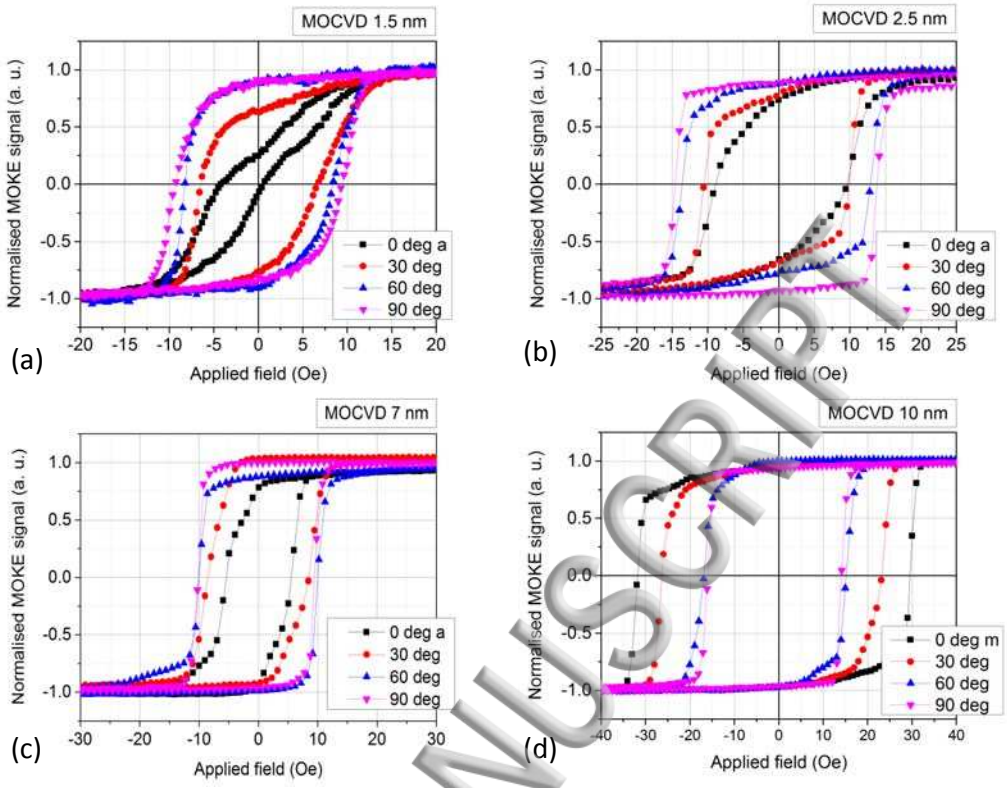


FIG. 8. Representative MOKE hysteresis plots of (a) 1.5 nm, (b) 2.5 nm, (c) 7 nm and (d) 10 nm Fe films. The *a* and *m* notations indicate *a*-axes $[11\bar{2}0]$ and *m*-axis $[1\bar{1}00]$ of GaN(0001).

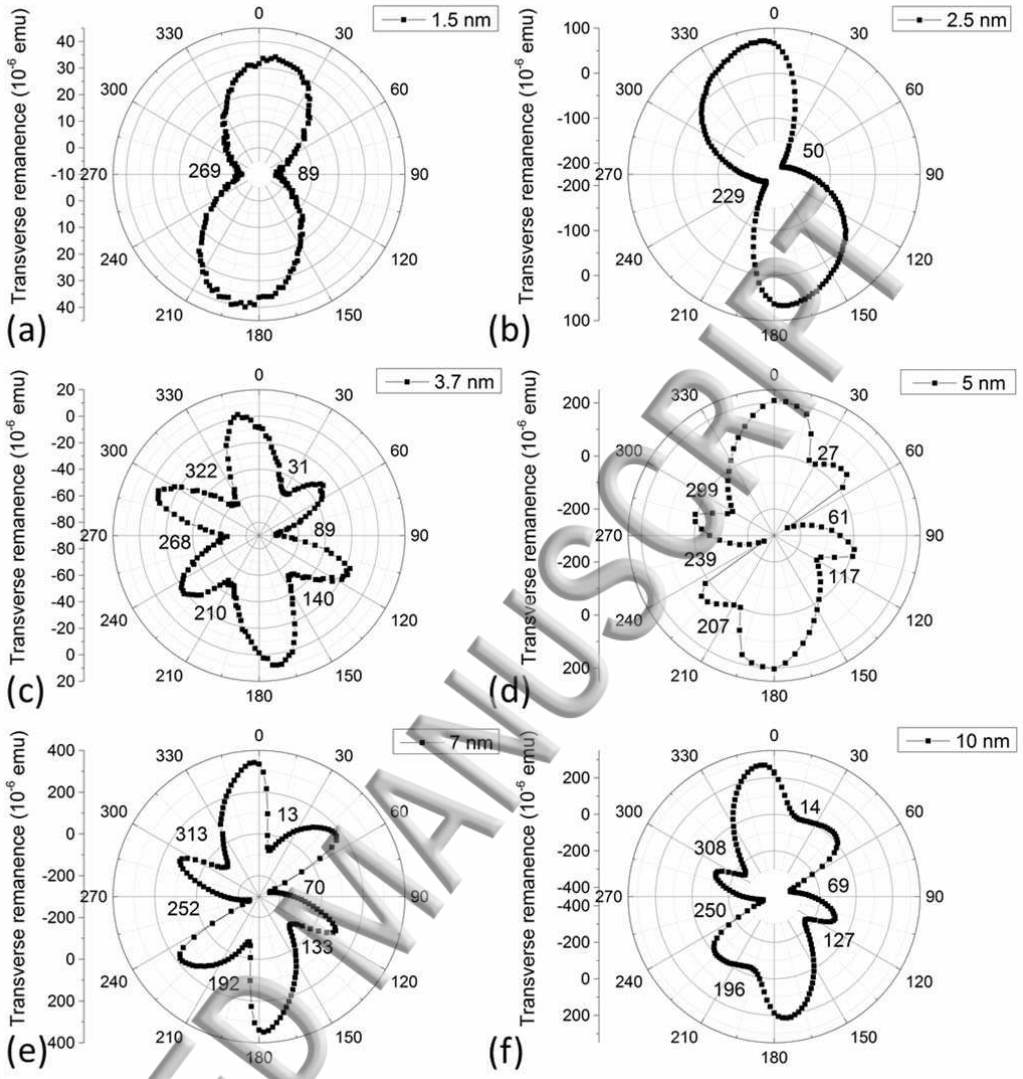


FIG. 9. Transverse components of remnant magnetisation plotted against sample angles for (a) 1.5 nm, (b) 2.5 nm, (c) 3.7 nm, (d) 5 nm, (e) 7 nm and (f) 10 nm. The numbers in the plots show the sample angles of minimum points. The zero degree aligns with the *a*-axis $[11\bar{2}0]$ of the GaN (0001).

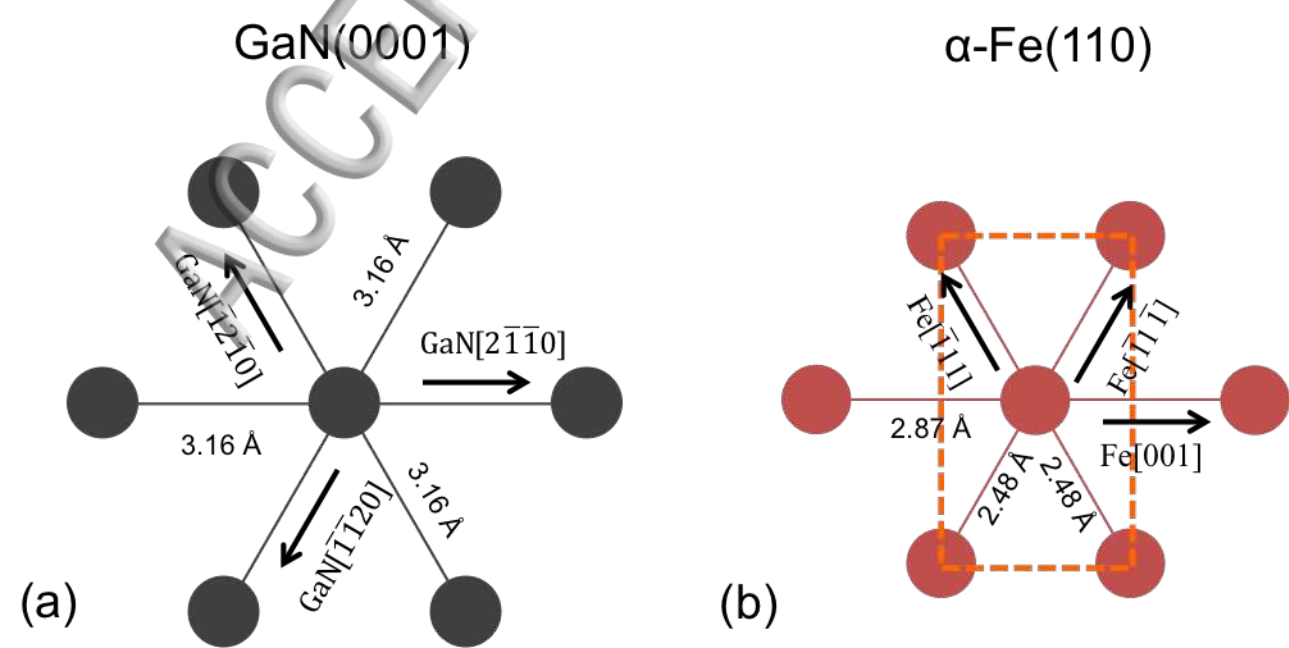
GaN(0001)
α-Fe(110)
GaN[$\bar{1}2\bar{1}0$]
3.16 Å
GaN[$2\bar{1}\bar{1}0$]
3.16 Å
GaN[$\bar{1}\bar{1}20$]
3.16 Å
(a)
Fe[$\bar{1}1$]
Fe[$\bar{1}\bar{1}$]
2.87 Å
Fe[001]
2.48 Å
2.48 Å
(b)

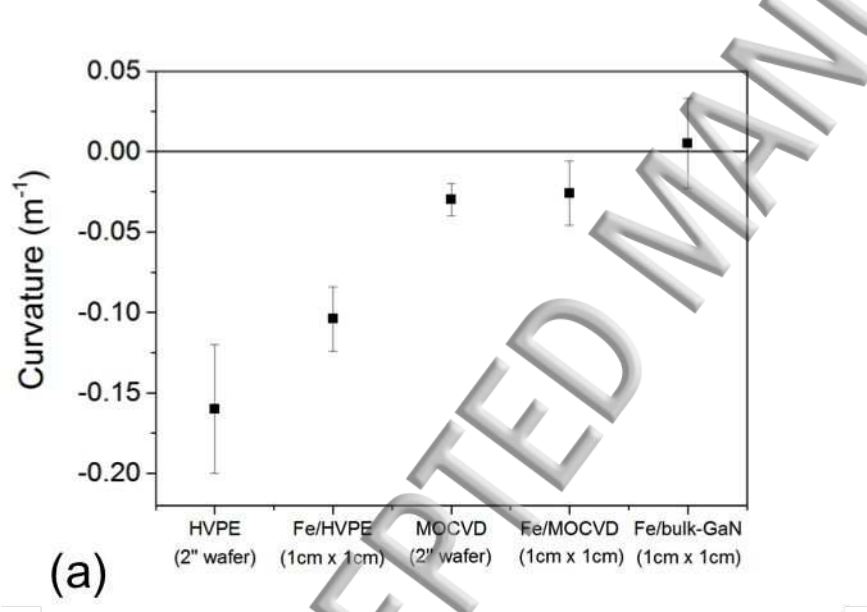


(a)

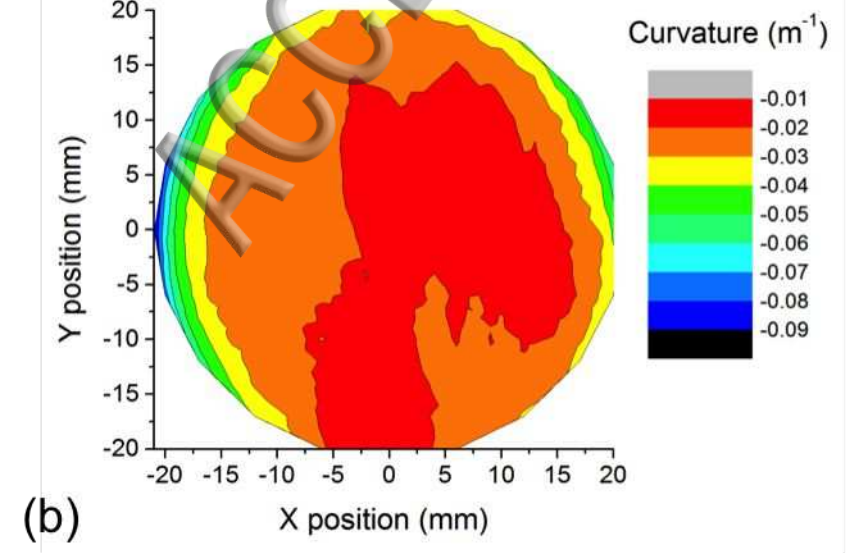


(b)

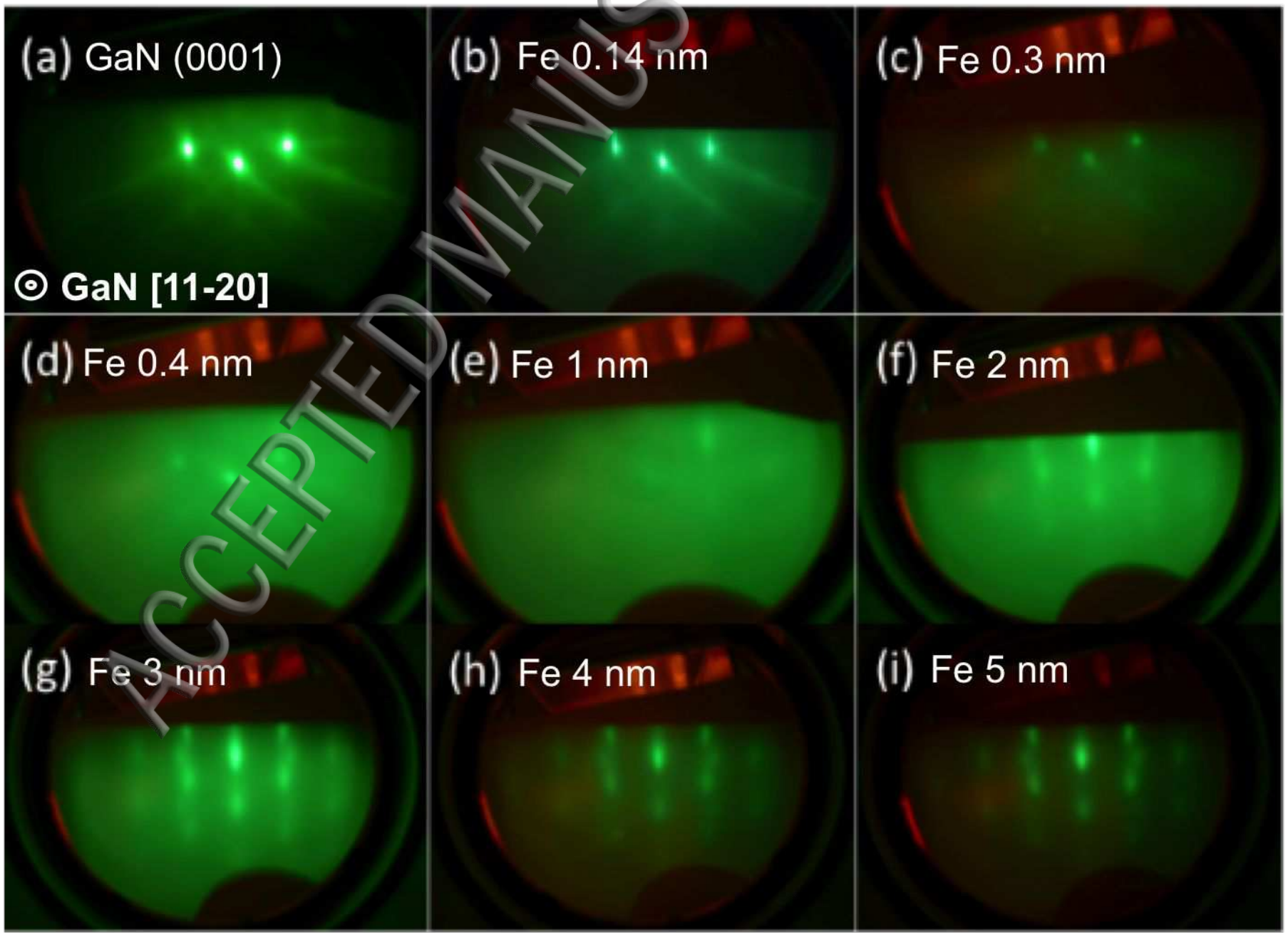

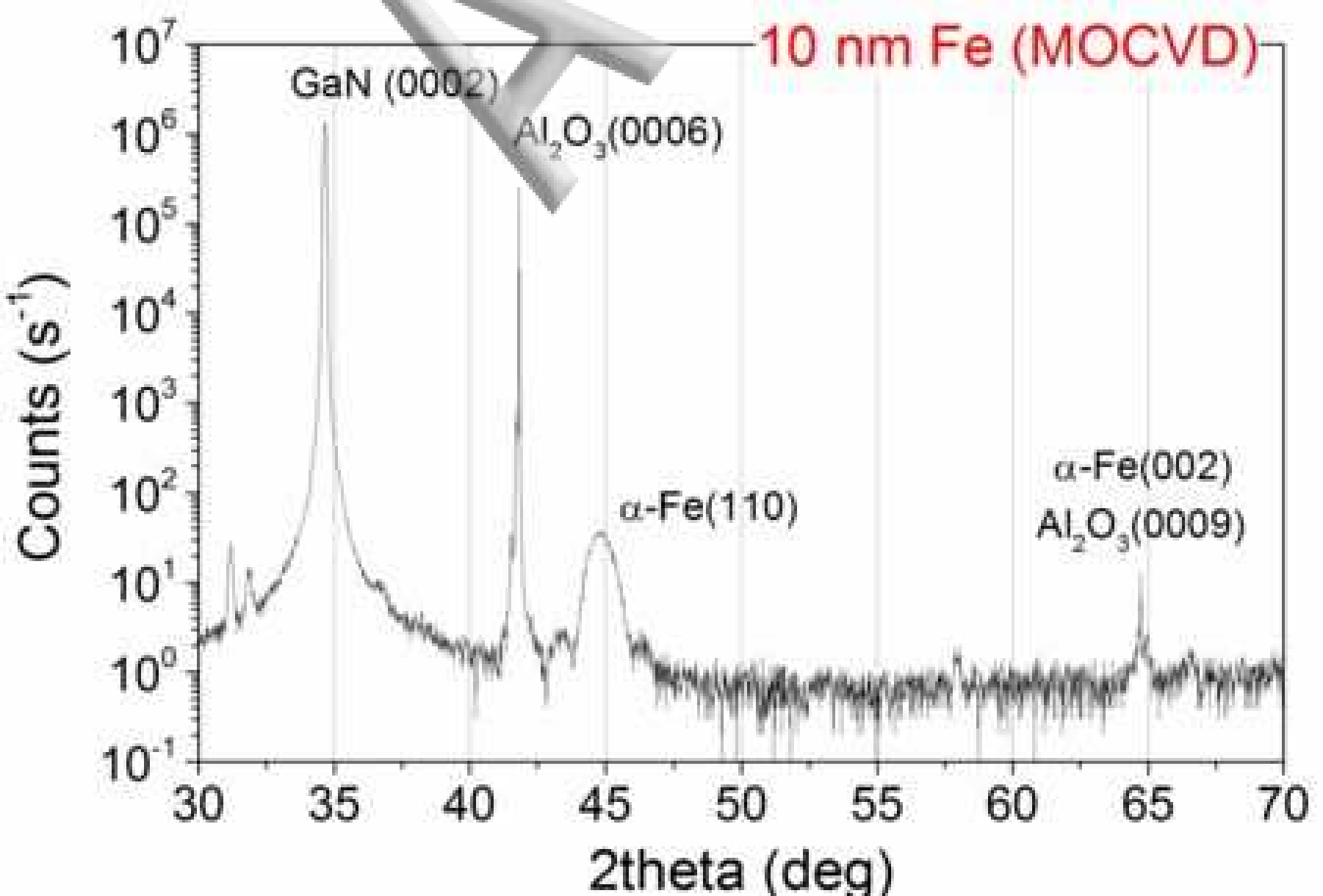
10 nm Fe (MOCVD)
GaN (0002)
Al2O3(0006)
α-Fe(110)
α-Fe(002)
Al2O3(0009)
Counts (s-1)
2theta (deg)
10^7
10^6
10^5
10^4
10^3
10^2
10^1
10^0
10^-1
30
35
40
45
50
55
60
65
70

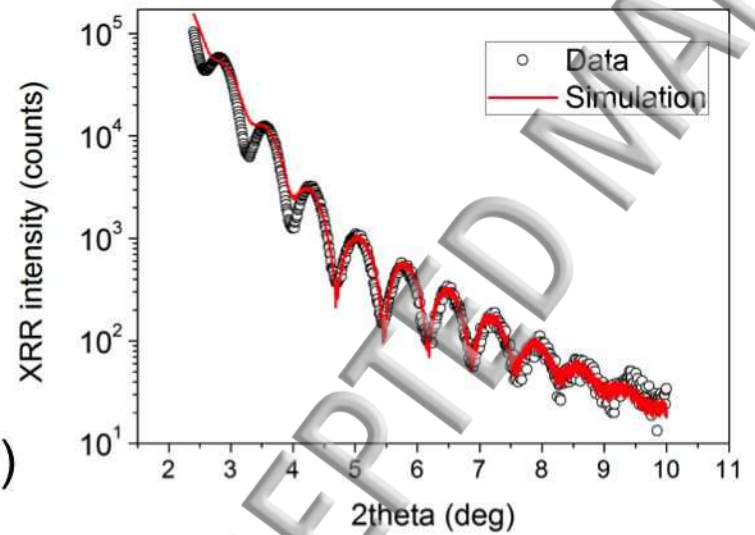


(a)

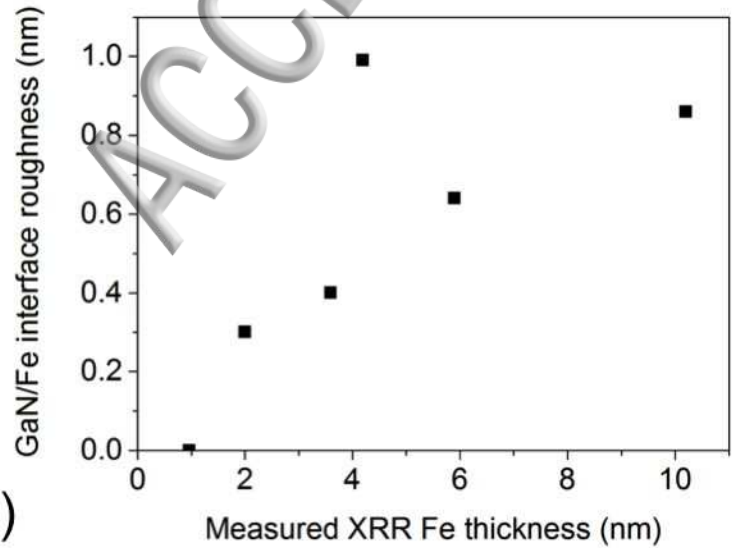


(b)

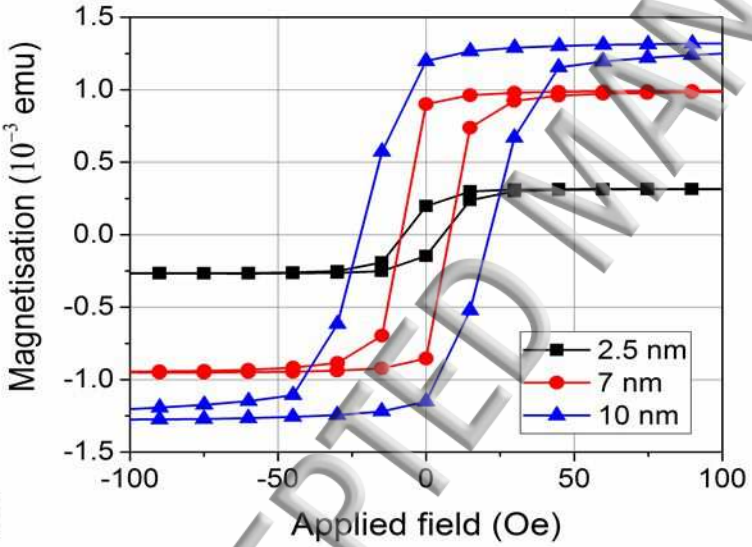


(a)

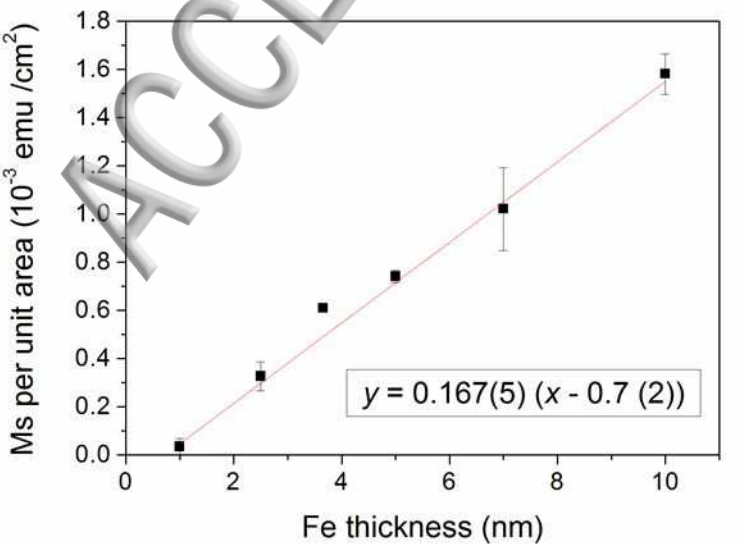


(b)

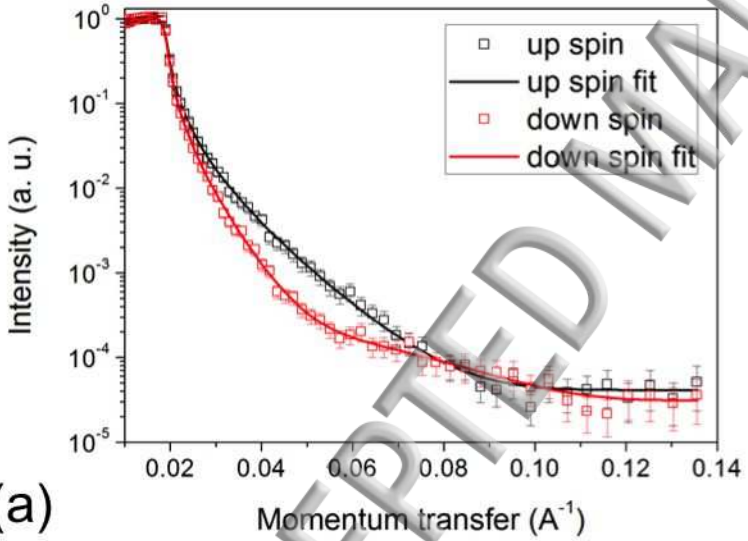


(a)

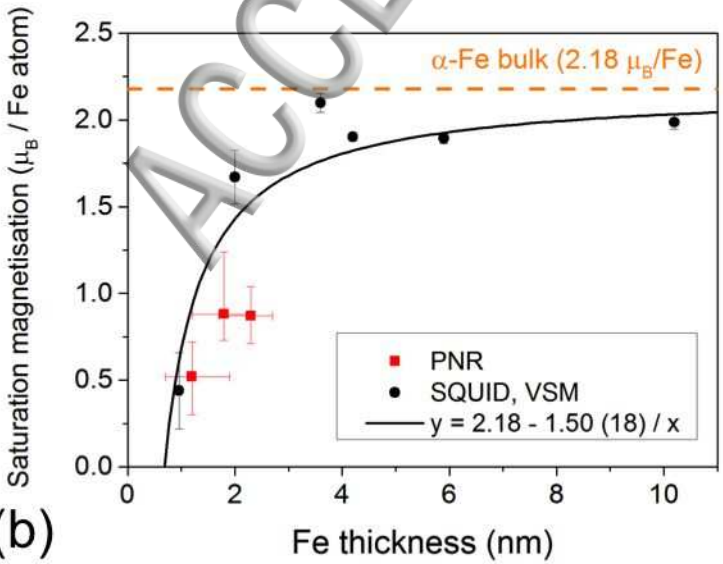


(b)